Available online at www.sciencedirect.com
ScienceDirect
Journal of the European Ceramic Society 31 (2011) 2981–2985
www.elsevier.com/locate/jeurceramsoc

Reducing the solubility of Ag into $BaTiO_3$ by alloying Ag with Pd

Shao-Ju Shih [a,*], Wei-Hsing Tuan [b]

[a] Department of Materials Science and Engineering, National Taiwan University of Science and Technology, Taipei 10607, Taiwan
[b] Department of Materials Science and Engineering, National Taiwan University, Taipei 10617, Taiwan

Received 19 November 2010; received in revised form 19 July 2011; accepted 24 July 2011
Available online 15 August 2011

Abstract

In the experiment reported in this study, a small amount of 70%Ag/30%Pd particles was mixed with $BaTiO_3$ powder and subsequently sintered at elevated temperature in nitrogen, air and oxygen. The solubility of Ag in the $BaTiO_3$ was determined using an electron probe microanalysis technique. The presence of Pd alloy in Ag can reduce its solubility and diffusion distance in $BaTiO_3$. Alloying with Ag significantly reduced the solubility of Pd in $BaTiO_3$.

Keywords: Solubility; $BaTiO_3$ and titanates; Inclusions; Capacitors; Electron microscopy

1. Introduction

Silver and silver/palladium alloys are frequently used as the inner electrode for $BaTiO_3$-based multi-layered capacitors. The inner electrode and the dielectric are co-fired at an elevated temperature to reach a dense laminated structure. A very small amount of Ag and Pd can dissolve into $BaTiO_3$ during cofiring.[1] Though the solubility of Ag in $BaTiO_3$ is low, the presence of Ag solute can enhance the grain growth rate of $BaTiO_3$.[2] Therefore, there is a need to reduce the solubility of Ag into $BaTiO_3$. Previous research claims that the addition of palladium alloy to silver can reduce its migration.[3] However, the effects of Pd alloy on the solubility of Ag in $BaTiO_3$ have not been investigated yet.

A reliable technique is needed first to determine the solubility. It is essential for the case of solution of Ag in $BaTiO_3$, for which the solubility level is low.[1] Researchers have employed several techniques to determine the solubility of Ag in dielectrics.[2,4,5] The most popular techniques involve the measurement of the Curie temperature[4,5] and lattice parameters.[2,5] However, the dielectric Curie temperature is affected by many factors, such as the presence of internal stress, external stress and microstructural characteristics.[6] When employing the X-ray diffraction (XRD) technique to determine lattice parameters, many specimens with various compositions have to be prepared first in order to determine the solubility. Furthermore, the change of lattice parameter is small when the solubility is low, which is the case for the solution of Ag in $BaTiO_3$.

An electron probe micro-analysis (EPMA) technique has been employed recently to determine the solubility of Ag or Pd in $BaTiO_3$. This technique first places the electron probe on one Ag inclusion. Spot analysis was then carried out across the entire inclusion into the matrix (Fig. 1(a)). The EPMA usually collects information from a pocket under the surface. The radius of each pocket is approximately 1 μm. The spots are therefore taken every micrometer from the inclusion. The intensity of solute is high when the electron beam hits the inclusion and subsequently reduces to a plateau (Fig. 1(b)). The height of the plateau indicates the solubility of the solute, while the width of the plateau in an indicator of the diffusion distance of the solute in the matrix. The EPMA intensity drops to zero when the solute is no longer detected. Though the solubility of Ag or Pd in $BaTiO_3$ is low, Table 1 shows that this technique can successfully determine their solubility. The scanned lines in Table 1 reveal the average value and standard deviation of the solubility. In addition, the microstructure of Ag/Pd-doped $BaTiO_3$ can be determined by backscatter electron images from scanning electron microscopy (SEM).

Since this technique has been successfully used to determine the solubility of Ag in $BaTiO_3$,[1] it can also determine the effects of Pd alloy on the solubility of Ag in $BaTiO_3$ This

* Corresponding author at: Department of Materials Science and Engineering, National Taiwan University of Science and Technology, Taipei 10607, Taiwan. Tel.: +886 2 27303716; fax: +886 2 27376544.
E-mail address: shao-ju.shih@mail.ntust.edu.tw (S.-J. Shih).

0955-2219/$ – see front matter.
doi:10.1016/j.jeurceramsoc.2011.07.031

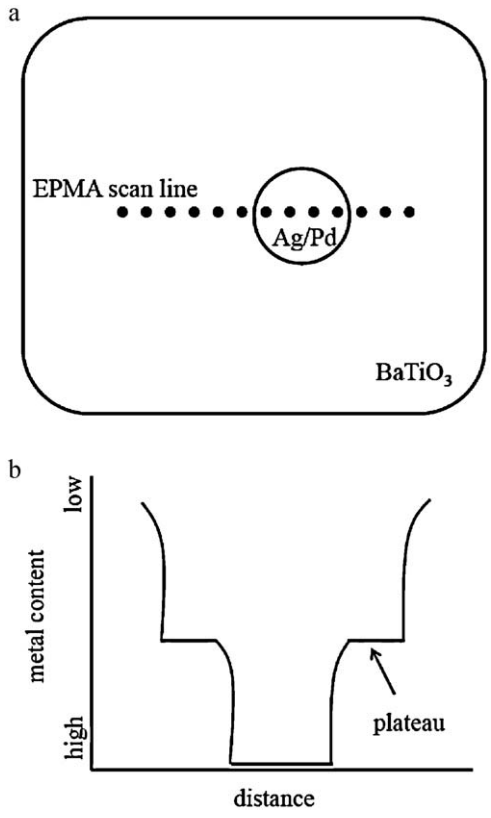

Fig. 1. Schematic of the EPMA technique[1] used to determine the solubility of the inclusion in matrix: (a) the scan line and (b) the examined curve.

study measured the solubility of Ag and Pd in $BaTiO_3$ for the 70%Ag/30%Pd doped $BaTiO_3$ is measured. The role of Ag to $BaTiO_3$, either as an acceptor or a donor, is also determined by firing the doped specimens in a sintering atmosphere with various oxygen partial pressures.

2. Experimental

$BaTiO_3$ powder (No. 219-6, Lot No. 2189-6, Ferro Co., Niagara Falls, NY, USA) was mixed with 1 wt% Ag/Pd powder (Shoei Chem. Inc., Japan) by ball milling in ethyl alcohol, using zirconia media for 24 h. The mean particle size of the $BaTiO_3$ powder was 1.2 μm; the Ba/Ti ratio was 0.995. The impurity levels were 910 ppm SrO, 600 ppm P_2O_5, 560 ppm SO_3, 500 ppm CaO, 180 ppm SiO_2, 170 ppm Na_2O, 160 ppm ZrO_2 and 150 ppm Al_2O_3, as reported by the manufacturer. According to the producer, the alloy contained 30% Pd. The slurry was dried and sieved through a No. 150 plastic mesh. Powder compacts of 10 mm in diameter and ~3 mm thick were formed by applying uniaxial pressure at 30 MPa. The resulting green density was ~54%. The sintering profile used was 1290 °C/2 h, with a heating rate of 3 °C/min and a cooling rate of 5 °C/min. The sintering atmospheres used were flowing air, nitrogen (~1 ppm O_2), and oxygen.

The vapor pressure of Ag is high at the temperature above the melting point of ~1210 °C for the Ag/Pd alloy (70%Ag/30%Pd),[7] creating a thin metal-depletion layer on the surface.[2,8] To minimize the influence of the metal-depletion layer, a surface layer ~0.5 mm thick was removed from the sintered specimens, using SiC sandpaper, before any measurements were taken. The final density was determined using the Archimedes method. Because the solubility of silver and the palladium in $BaTiO_3$ is low, the theoretical density of silver-doped $BaTiO_3$ was estimated using 6.02 g/cm^3 for $BaTiO_3$ and 10.96 g/cm^3 for 70%Ag/30%Pd alloy. The polished surface was prepared by grinding with SiC particles and polishing with Al_2O_3 particles. Grain boundaries were revealed by etching with an aqueous solution of HCl and HF that was dilute enough to leave the alloy inclusions intact. The microstructure was observed using optical microscopy and scanning electron microscopy. For SEM (JSM6510, JEOL, Tokyo, Japan), backscatter electron images were captured to enhance the contrast between the inclusions of Ag/Pd alloy and the $BaTiO_3$ matrix. Phase identification was performed using XRD at a scanning rate of 0.05° 2θ/s.

An EPMA (Model JAX-8600SX, JEOL, Tokyo, Japan) was used under the operation conditions of 15 kV and 1×10^{-7} A with an electron probe spot size of 1.5 μm. The specimens were polished before measurement. An undoped $BaTiO_3$ specimen was used as a reference. One Ag/Pd inclusion in the $BaTiO_3$ matrix was located first, then the electron probe was spotted every micrometer along a straight line from the chosen inclusion. Approximately 20 points (a distance of 20 μm) were measured. For each sample, five to ten scanned lines were chosen randomly. Therefore, more than 100 points were measured for each composition.

Table 1
Solubility of Ag and Pd in $BaTiO_3$ as only Ag or only Pd particles were added into $BaTiO_3$. The values were determined using the EPMA technique.

	Sintering atmosphere		
	N_2	Air	O_2
Ag			
Solubility/ppm	200 ± 70	450 ± 70	1000 ± 40
Diffusion distance/μm	3	>5	>5
Pd			
Solubility/ppm	0	50 ± 20	300 ± 70
Diffusion distance/μm	N.D.[a]	N.D.[a]	N.D.[a]

[a] N.D. = not determined. It is mainly due to that the diffusion distance is around or smaller than 1 μm, which is below the detection limit of the EPMA technique used.

3. Results and discussion

The X-ray diffraction pattern for the starting Ag/Pd powder reveals distinct silver and palladium peaks, indicating that Ag and Pd particles are physically mixed in the starting material (Fig. 2). The Pd began to oxidize from a temperature around 250 °C and subsequently reduced to its metallic form and solution with Pd to form Ag–Pd alloy at 450 °C.[9] Using a high-temperature XRD experiment, Wang et al. reported that Pd forms a PdO phase from 200 to ~680 °C and reduces to Pd for Ag–Pd alloy above ~680 °C in air.[3] Therefore, Ag and Pd formed alloy well before the start of sintering. After sintering at 1290 °C, XRD analysis reveals only $BaTiO_3$ in the Ag/Pd-doped

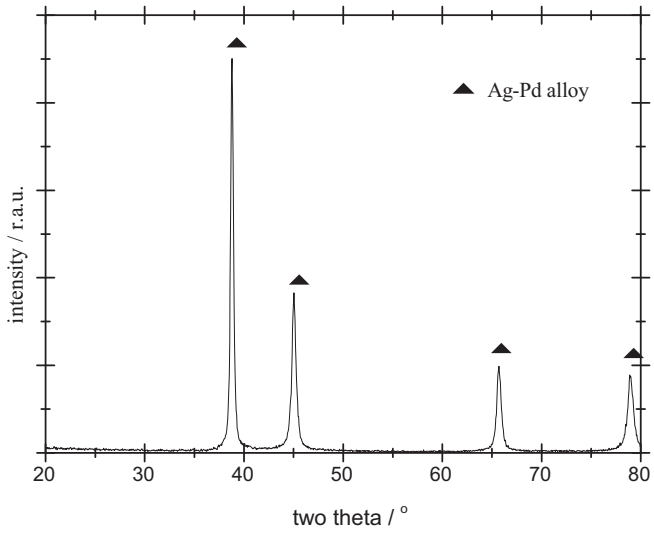

Fig. 2. The XRD pattern of the Ag/Pd starting powder.

$BaTiO_3$. This is mainly because the amount of Ag/Pd alloy is low. The relative density of the specimen after sintering in different atmosphere varied within a very narrow range from 97.3% to 98.2% (Table 2). The average size of Ag/Pd alloy inclusions was 0.7 μm.

Fig. 3 shows a backscatter electron image of the Ag/Pd doped $BaTiO_3$ specimen. The distribution of the Ag/Pd inclusions is not uniform because the amount of the Ag/Pd inclusions is small (1 wt% or 0.6 vol.%). Since the Ag/Pd inclusions are well separated from each other, they do not affect the EPMA analysis. Fig. 4 shows typical EPMA result for the specimen sintered in air. Two alloy inclusions were spotted within a distance of 15 μm. The intensity of Ag at the alloy inclusion is very high, and then drops to a saturated value. The height of the plateau indicates the solubility of Ag in $BaTiO_3$. The solubility of Ag in $BaTiO_3$ for this specific case is 267 ppm. The width of the plateau is approximately 6 μm, indicating that the diffusion distance of Ag in $BaTiO_3$ is longer than 3 μm (Table 2). Fig. 4 shows no plateau found for the Pd curve. This suggests that the solubility of Ag in $BaTiO_3$ is very low and the diffusion distance of Pd in $BaTiO_3$ is short. Table 2 shows the average value

Table 2
Relative density and solubility of Ag and Pd in $BaTiO_3$ as 70Ag/30Pd particles were added. The values were determined using the EPMA technique.

	Sintering atmosphere		
	N_2	Air	O_2
Relative density/%	97.5 ± 0.1	98.2 ± 0.1	97.3 ± 0.2
Ag			
Solubility/ppm	0	260 ± 120	240 ± 80
Diffusion distance/μm	N.D.[a]	~3	~5
Pd			
Solubility/ppm	~30	~0	~20
Diffusion distance/μm	N.D.[a]	N.D.[a]	N.D.[a]

[a] N.D. = not determined. It is mainly due to that the diffusion distance is around or smaller than 1 μm, which is below the detection limit of the EPMA technique used.

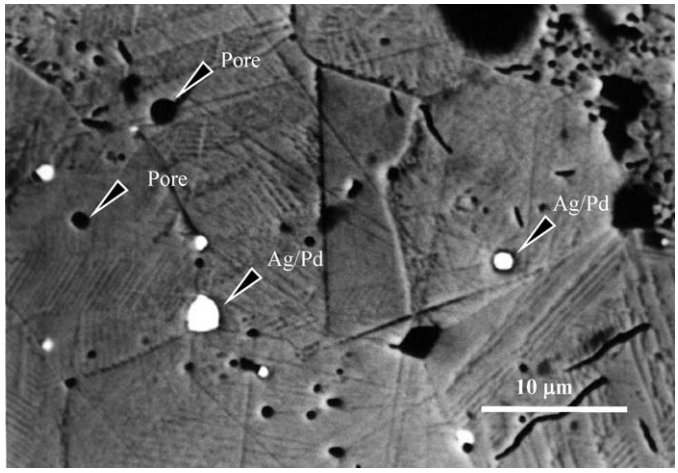

Fig. 3. Typical microstructure of the Ag/Pd doped $BaTiO_3$ specimen sintered in air, with some Ag/Pd inclusions indicated.

of the solubility derived from several scanned lines along with the diffusion distance.

Fig. 5 shows a typical result for the Ag/Pd doped $BaTiO_3$ sintered in nitrogen. The no plateau was, indicating that the solubility of Ag in $BaTiO_3$ is negligible (Table 2). The solubility of Pd in $BaTiO_3$ is also low, at approximately 30 ppm.

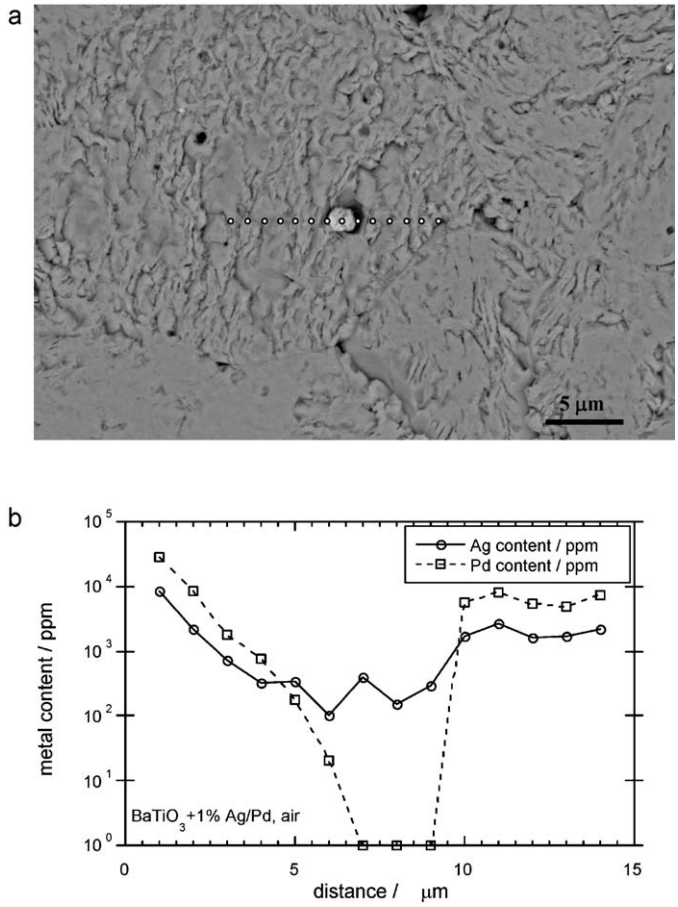

Fig. 4. (a) The backscatter electron image and (b) the EPMA analysis curve (from the dashed line in (a)) of the 70Ag/30Pd particle embedded in Ag/Pd doped $BaTiO_3$ sintered in air.

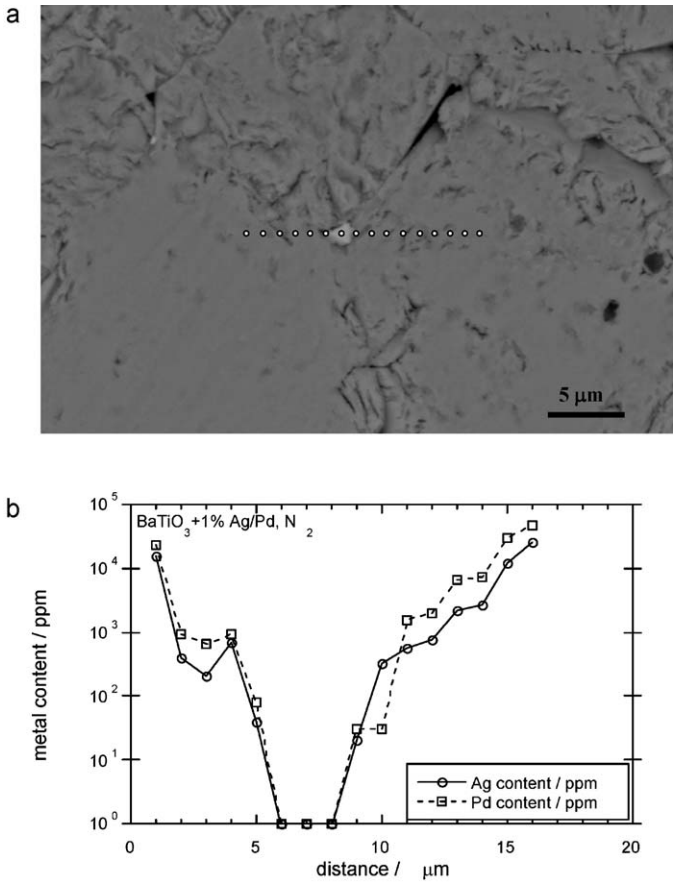

Fig. 5. (a) The backscatter electron image and (b) the EPMA analysis curve (from the dashed line in (a)) of the 70Ag/30Pd particle embedded in Ag/Pd doped $BaTiO_3$ sintered in nitrogen.

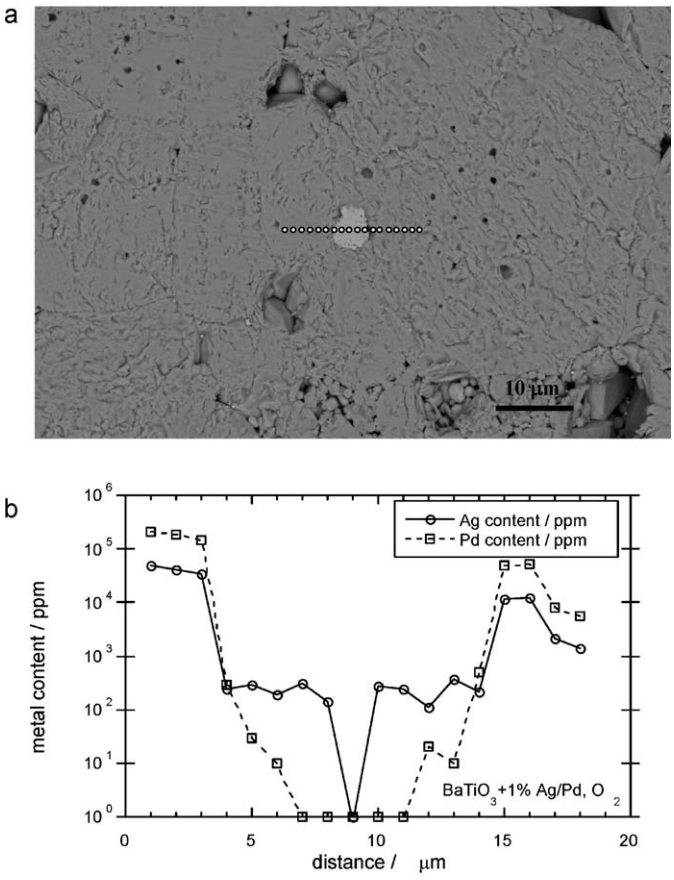

Fig. 6. (a) The backscatter electron image and (b) the EPMA analysis curve (from the dashed line in (a)) of the 70Ag/30Pd particle embedded in Ag/Pd doped $BaTiO_3$ sintered in oxygen.

This value is close to the detection limit of the system, indicating that the solution of Pd in $BaTiO_3$ is also very small (Table 2). Fig. 6 shows a typical intensity–distance curve for the 70Ag/30Pd-doped $BaTiO_3$ sintered in oxygen. The solubility of Ag in $BaTiO_3$ is approximately 240 ppm for the specific case shown in this figure. The diffusion distance is around 5 μm (Table 2). The solubility of Pd in $BaTiO_3$ is also low, which is approximately 20 ppm.

The solubility of the acceptor can be suppressed as $BaTiO_3$ is fired in a reducing atmosphere.[10] The solubility of Ag in $BaTiO_3$ decreased significantly as the specimen was sintered in nitrogen, suggesting that Ag ion acts as the acceptor for $BaTiO_3$. The Ag^+ and Ba^{2+} ions are similar in size[11] (Table 3). Though they differ in ionic charge, Ag^+ tends to substitute Ba^{2+} and is compensated by a corresponding number of oxygen vacancy as follows

$$2Ag = 2Ag'_{Ba} + V_o^{\bullet\bullet} \quad (1)$$

Table 3
Ionic radii of Ag^+, Pd^{2+}, Ba^{2+} and Ti^{4+} ions as reported in the literature.[11]

Ag^+	Pd^{2+}	Ba^{2+}	Ti^{4+}
0.149 nm	0.086 nm	0.135 nm	0.061 nm

The decrease of oxygen partial pressure in sintering atmosphere can also induce the formation of oxygen vacancy as follows

$$O_o = \frac{1}{2}O_2 + V_o^{\bullet\bullet} + 2e' \quad (2)$$

Reaction (2) seems to dominates the solution process, as the reduction of oxygen partial pressure increases the concentration of oxygen vacancy. Reaction (1) is suppressed according to Le Chatelier's principle. The Ag ion solution therefore decreased when the specimen sintered in nitrogen, which creating the oxygen partial pressure of approximately 1 ppm. The Pd^{4+} ion acts the acceptor to as only Pd is doped into $BaTiO_3$.[1] This is because the ionic radius of Pd^{2+} is similar to that of Ti^{4+} (Table 3). It is also possible that Pd ion replaces Ti ion during cofiring of Ag/Pd doped $BaTiO_3$, as the following reaction,

$$Pd = Pd''_{Ti} + V_o^{\bullet\bullet} \quad (3)$$

The solubility of Pd into $BaTiO_3$ is extremely low for the present system. Therefore, it is hard to justify the role of the Pd ion to $BaTiO_3$. Nevertheless, the Pd ion may still act as acceptor if any Pd is dissolved in $BaTiO_3$.

The solubility of Ag in the Ag/Pd-doped $BaTiO_3$ (Table 2), is lower than that of Ag in the Ag-doped $BaTiO_3$ (Table 1). The solubility of Pd is also lower than that of Pd in the Pd-doped $BaTiO_3$ system. Both Ag and Pd act as acceptors for $BaTiO_3$.

The replacement of Ag^+ ion with Ba^{2+} seems easier than that of Pd^{2+} with Ti^{4+}. It may be because the replacement of Ag^+ with Ba^{2+} introduces strain into the crystal structure, inhibiting further insertion of Pd^{2+} ions into the structure. This significant reduces the solubility of Pd. The solution of a very small amount of Pd^{2+} can always reduce the solution ability of Ag^+ into the structure, suppressing the solubility of Ag^+ in $BaTiO_3$. Note that the diffusion distance of Ag in $BaTiO_3$ also reduces. This may be related to the reduction of Ag solution in $BaTiO_3$.

4. Conclusions

Both Ag and Pd act as acceptors for $BaTiO_3$. The solution of one acceptor can reduce the solution of another acceptor. Therefore, the solution of Ag in $BaTiO_3$ (Ag solubility of 200 ± 70 ppm, 450 ± 70 ppm and 1000 ± 40 ppm in nitrogen, air and oxygen, respectively) is reduced when Ag is alloyed with Pd before sintering (Ag solubility of 0 ppm, 260 ± 120 ppm and 240 ± 80 ppm in nitrogen, air and oxygen, respectively). The lower solubility of Ag in $BaTiO_3$ also reduces the diffusion distance of Ag in $BaTiO_3$.

Acknowledgements

The authors would like to thank the National Science Council, Republic of China, for its financial supports under contract No. NSC92-2216-E002-029 and NSC99-2218-E-011-030-MY2.

References

1. Shih SJ, Tuan WH. Solubility of silver and palladium in $BaTiO_3$. *J Am Ceram Soc* 2004;**87**:401–7.
2. Chen CY, Tuan WH. Effect of silver on the sintering and grain-growth behavior of barium titanate. *J Am Ceram Soc* 2000;**83**:2988–92.
3. Wang SF, Dougherty JP, Huebner W, Pepin JG. Silver–palladium thick-film conductors. *J Am Ceram Soc* 1994;**77**:3051–72.
4. Ikushima H, Hayakawa S. Electrical properties of Ag-doped barium titanate ceramics. *Jpn J Appl Phys* 1965;**4**:328–36.
5. Sato Y, Kanai H, Yamashita Y. Effects of silver and palladium doping on the dielectric properties of $0.9Pb(Mg_{1/3}Nb_{2/3})O_3$–$0.1\ PbTiO_3$ ceramic. *J Am Ceram Soc* 1996;**79**:261–5.
6. Hwang HJ, Nagai T, Ohji T, Sando M, Toriyama M, Niihara K. Curie temperature anomaly in lead zirconate titanate/silver composites. *J Am Ceram Soc* 1998;**81**:709–12.
7. Karakaya I, Thompson W. The Ag–Pd (silver–palladium) system. *J Phase Equilib* 1988;**9**:237–43.
8. Panteny S, Bowen CR, Stevens R. Characterisation of barium titanate–silver composites, part I: microstructure and mechanical properties. *J Mater Sci* 2006;**41**:3837–43.
9. Cole SS. Oxidation and reduction of palladium in the presence of silver. *J Am Ceram Soc* 1985;**68**:C-106–7.
10. Bheemineni V, Chang EK, Lal M, Harmer MP, Smyth DM. Suppression of acceptor solubilities in $BaTiO_3$ densified in highly reducing atmospheres. *J Am Ceram Soc* 1994;**77**:3173–6.
11. Shannon RD. Revised effective ionic radii and systematic studies of interatomic distances in halides and chalcogenides. *Acta Crystallogr A Found Crystallogr* 1976;**32**:751–67.